Heisenberg Spin Chains and DMRG

Lucas Z. Brito

June 16, 2022

Contents

1 Introduction

The simplification that occurs when reducing the dimensionality of a physical model is practically a secondhand intuition to practicing physicists: systems tend to become much more intuitive, visualizable, and tractable upon simplification from three dimensions to two or even one. This is especially the case in quantum many body physics, a field which by nature tackles exponentially complex problems. Reduction in spatial dimension then becomes a stepping stone for condensed matter and quantum many body physicists to get a handle on models which otherwise would be too formidable to be approached. Remarkably, however, it is often the case the the restrictive nature of one or two-dimensional systems in fact leads to surprising and exotic physics (as in the case of anyons)—and that, as is often the case in condensed matter physics, such systems are fully experimentally realizable in all of their bizarreness.

In this paper we introduce and motivate an important example of physics in one-dimension, the *Heisenberg spin chain*. The Heisenberg spin chain is an important model for understanding (anti)ferromagnetism, quantum spin liquids, spin-wave excitations, and, notably has been successfully prepared in laboratory settings [5]. In Section 2 we define the Heisenberg spin chain Hamiltonian and briefly discuss its variations, and in Section 3 we discover the remarkable fact that the Heisenberg spin chain Hamiltonian can be recovered as an effective Hamiltonian of the *Hubbard model*. Having understood the Heisenberg model and properly motivated it, in Section 4 we introduce a technique that has become enormously popular in solving spin chain problems, the *density matrix renormalization group* (DMRG) approach; Section 4.1 details the more modern view of DMRG as it relates to the rich study of *tensor networks*. Finally, Section 4.2 displays the results of DMRG applied to a Heisenberg spin chain as compared to the groundstate energy prediction of the Bethe ansatz.

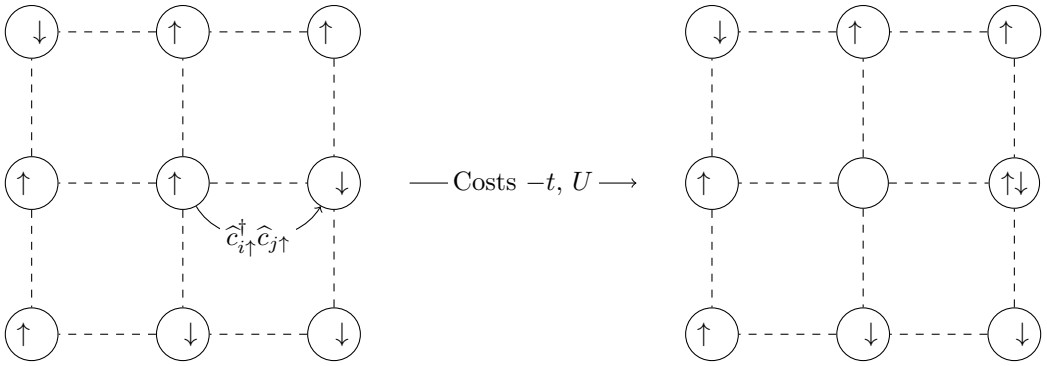

Figure 1: Diagram of a hop in the Hubbard model with half-filling $\langle \hat{n}_{i\uparrow} + \hat{n}_{i\downarrow} \rangle = 1$. Here we have a spin up electron hopping from the middle site to the right-middle site. This costs a double occupation penalty U.

2 The Quantum Heisenberg Model

The (quantum[1]) Heisenberg model is

$$\hat{H} = -\sum_{\langle ij \rangle} \hat{\boldsymbol{\sigma}}_i \cdot (J\hat{\boldsymbol{\sigma}}_j) = -\sum_{\langle ij \rangle} \left[J_x \hat{\sigma}^x_i \hat{\sigma}^x_j + J_y \hat{\sigma}^y_i \hat{\sigma}^y_j + J_z \hat{\sigma}^z_i \hat{\sigma}^z_j \right]$$

where $\hat{\boldsymbol{\sigma}}_i$ is a Pauli vector operator acting on the i-th Hilbert space, J is a diagonal matrix which contains the coupling constants for each direction $J_{x,y,z}$, and $\langle ij \rangle$ denotes adjacent pairs of sites in an arbitrary lattice. If we introduce an external magnetic field, the Hamiltonian simply acquires a new term:

$$\hat{H} = -\sum_{\langle ij \rangle} \hat{\boldsymbol{\sigma}}_i \cdot (J\hat{\boldsymbol{\sigma}}_j) + h \sum_i \hat{\sigma}^x_j$$

Depending on the choice of $J_{x,y,z}$, this Hamiltonian will fall into different subclasses of Heisenberg models; choosing $J_x = J_y = J_z$, for example, obtains the Heisenberg XXX model, where $J_x = J_y \neq J_z$ obtains the XXZ model. If we choose our lattice to be a one-dimensional "string" of particles, our model is termed a *spin chain*.

The Heisenberg model is an oft-cited one because it captures local spin-spin couplings in a simple way and thus can be used to model ferromagnetism and antiferromagnetism. In particular, if we choose an XXX model in the absence of a magnetic field, the model becomes

$$\hat{H} = -J \sum_{\langle ij \rangle} \hat{\boldsymbol{\sigma}}_i \cdot \hat{\boldsymbol{\sigma}}_j$$

(where J_x has been abbreviated to J). Here it is salient that the sign of the coupling constant will largely determine the behavior of the system: a negative J energetically punishes spin alignment, whereas a positive J favors it.

3 Spin Chains from the Hubbard Model

While the Heisenberg model is typically introduced as a purely heuristic Hamiltonian used to model ferromagnetism, one can follow a derivation that remarkably explains its spin-spin couplings as emerging from electron repulsion and exchange statistics. Although this story starts with the Coulomb-interaction-only *Hubbard model*, we will obtain an identical-form Heisenberg spin chain as a low-energy "effective Hamiltonian"; in this sense, the Heisenberg model is nothing more than a tight-binding electron lattice viewed in a particular regime.[2]

[1] There exists a classical Heisenberg model which we do not discuss here.

[2] This derivation of spin chains is due to Girvin and Yang, *Modern Condensed Matter Physics* (2019) [3].

The Hubbard model describes a lattice accommodating Coulomb interactions and nothing more. There are two terms in the Hamiltonian: one which encourages hopping between nearest-neighbor sites (roughly characterizing the kinetic energy of the system) and one which energetically punishes doubly occupied lattice sites (analogously to a potential representing Coulomb repulsion). If we parameterize the hopping tendency by t and the cost of double-occupation by U, the Hamiltonian is, in the second quantization formalism,

$$\widehat{H} = -t \sum_{\langle ij\rangle,\sigma} \left(\widehat{c}^\dagger_{i\sigma}\widehat{c}_{j\sigma} + \widehat{c}^\dagger_{j\sigma}\widehat{c}_{i\sigma}\right) + U\sum_j \widehat{n}_{j\uparrow}\widehat{n}_{j\downarrow}$$

where $\sigma \in \{\uparrow,\downarrow\}$, $\widehat{n}_{i\sigma} \equiv \widehat{c}^\dagger_{i\sigma}\widehat{c}_{i\sigma}$ and $\langle ij\rangle$ denotes nearest-neighbor site pairs.[3] At a high level, we expect the behavior of the system to depend on two degrees of freedom: the *band filling* $\langle \widehat{n}_{j\uparrow} + \widehat{n}_{j\downarrow}\rangle \in [0,2]$[4], and the ratio U/t. Indeed, the physics will entirely depend on our choices of these parameters. See Figure 1 for a diagrammatic representation of this model.

With this understanding, we choose a "half-filling" $\langle \widehat{n}_{j\uparrow} + \widehat{n}_{j\downarrow}\rangle = 1$, and $|U/t|$ large $\implies U \gg |t|$, such that the same-site repulsion is considerably stronger than the kinetic energy of the system. In this regime, we expect low-energy states to admit only single occupation and double occupation to only occur in a high-energy state; it is this intuition that poises us to employ perturbation theory and obtain our promised effective Hamiltonian $\widehat{H}_{\text{eff}}$. The idea is to "decouple" the low energy and high energy states by eliminating (through a suitable transformation) transitions between those two energy regimes; in doing so, we will obtain "disconnected" high energy and low energy Hamiltonians, out of which we will pick the low energy $\widehat{H}_{\text{eff}}$. To this end, our suitable transformation becomes the *Schrieffer-Wolff transformation*, which will, to first order in $1/U$ (i.e., to good approximation in the low-energy regime) diagonalize the Hamiltonian, successfully decoupling the low and high energy sectors [2].

The Schrieffer-Wolff transformation requires a perturbed Hamiltonian of the form $\widehat{H}_0 + \widehat{H}_1$, where $\widehat{H}_1$ is assumed to be off-diagonal in the eigenstates of the unperturbed Hamiltonian.[5] In the case of the Hubbard model, we will use

$$\widehat{H} = \widehat{T} + \widehat{V}, \quad \widehat{V} = U\sum_j \widehat{n}_{j\uparrow}\widehat{n}_{j\downarrow}, \quad \widehat{T} = -t\sum_{\langle ij\rangle,\sigma}\left(\widehat{c}^\dagger_{i\sigma}\widehat{c}_{j\sigma} + \widehat{c}^\dagger_{j\sigma}\widehat{c}_{i\sigma}\right) \equiv \widehat{T}_0 + \widehat{T}_+ + \widehat{T}_-$$

where $T_{+,-,0}$ change the number of doubly occupied sites by 1, -1, or zero respectively. Commutation relations for these operators can be obtained by studying their effects on a state $|n\rangle$ with n doubly-occupied sites:

$$[\widehat{V},\widehat{T}_m]\,|n\rangle = \widehat{V}\widehat{T}_m\,|n\rangle - \widehat{T}_m\widehat{V}\,|n\rangle = (n+Um)\,|n+m\rangle - Un\,|n+m\rangle \tag{1}$$

$$= Um\,|n+m\rangle = Um\widehat{T}_m\,|n\rangle \implies [\widehat{V},\widehat{T}_m] = Um\widehat{T}_m \tag{2}$$

Now we prepare our Hamiltonian in a fashion opposite to typical perturbation theory: in the $U \gg |t|$ regime the perturbative term is the kinetic one. One caveat is that we expect $\widehat{T}_0$ to have diagonal elements in the eigenbasis of $\widehat{T}$ as it definitionally leaves the double occupation number unchanged. This will introduce incompatibility with the Schrieffer-Wolff transformation; to ameliorate the perturbation we make the slight adjustment to our unperturbed/perturbed Hamiltonians:

$$\widehat{H}_0 \equiv \widehat{V} + \widehat{T}_0, \quad \widehat{H}_1 \equiv \widehat{T}_+ + \widehat{T}_-$$

With the perturbation properly arranged, the core idea of the Schrieffer-Wolff transform is to perform a transformation such that first-order appearances of the perturbative term vanish; in doing so, we will find that

[3] Note how readable the Hamiltonian becomes by choosing to write it in second quantization. Also note that the two terms for each $\langle ij\rangle$ do *not* necessarily represent an electron exchange; it is just pithy notation used to capture hops from i to j as well as from j to i.

[4] Roughly speaking, this describes how many electrons we've stuffed in the lattice, per site. The upper bound is enforced by the Pauli exclusion principle. Note the spins are opposite.

[5] As it turns out, one can always choose this to be the case by subtracting diagonal matrix elements from $\widehat{V}$ and incorporating them into $\widehat{H}_0$.

the transformed Hamiltonian becomes block diagonal in each energy sector and thus the low energy effective Hamiltonian is easily obtained by choosing the appropriate block. We know that for the transformation to be unitary (for us to not lose any information when we find the effective Hamiltonian), its operator must be some

$$\widehat{W} = \exp\Big(\widehat{S}\Big) \quad \text{with} \quad \widehat{S}^\dagger = \widehat{S}.$$

Starting with this form, we will proceed with the transformation to find further constraints on the generator $\widehat{S}$. The new Hamiltonian will be

$$\widehat{H}' = e^{\widehat{S}}\widehat{H}e^{-\widehat{S}} = \widehat{H} + [\widehat{S},\widehat{H}] + \frac{1}{2}[\widehat{S},[\widehat{S},\widehat{H}]] + \cdots$$

under the Baker-Campbell-Hausdorff expansion. Substituting $\widehat{H} = \widehat{H}_0 + \widehat{H}_1$ we find

$$\widehat{H}' = \widehat{H}_0 + \widehat{H}_1 + [\widehat{S},\widehat{H}_0] + [\widehat{S},\widehat{H}_1] + \frac{1}{2}[\widehat{S},[\widehat{S},\widehat{H}_0]]\cdots$$

Which immediately produces the constraint

$$[\widehat{S},\widehat{H}_0] = -\widehat{H}_1 \tag{3}$$

Provided we can find a generator satisfying the above, the transformed Hamiltonian is

$$\widehat{H}' = \widehat{H}_0 + \frac{1}{2}[\widehat{S},\widehat{H}_1] + O(\widehat{H}_1^3) \tag{4}$$

because $[\widehat{S},[\widehat{S},\widehat{H}_0]] = -[\widehat{S},\widehat{H}_1]$. To see why this will decouple the Hamiltonian as promised, define projector operators onto the low and high energy sectors $\widehat{P}_{l,h}$. A (block) diagonal operator in the low and high energy sectors can be expressed by $\widehat{A} = \widehat{P}_l\widehat{A}\widehat{P}_l + \widehat{P}_h\widehat{A}\widehat{P}_h$, whereas an off-diagonal operator is written $\widehat{A} = \widehat{P}_l\widehat{A}\widehat{P}_h + \widehat{P}_l\widehat{A}\widehat{P}_h$ and an arbitrary operator is a sum of these two components. Now, we can now show that we have freedom to choose a completely off-diagonal $\widehat{S}$ satisfying (3); all we have to do is additively decompose $\widehat{S}$ into a component $\widehat{S}_{\text{off}}$ off-diagonal in the eigenbasis of $\widehat{H}_0$ and a component $\widehat{S}_{\text{diag}}$ diagonal in the same basis. From here we see (3) becomes

$$[\widehat{S}_{\text{diag}},\widehat{H}_0] + [\widehat{S}_{\text{off}},\widehat{H}_0] = -\widehat{H}_1 \Longrightarrow [\widehat{S}_{\text{off}},\widehat{H}_0] = -\widehat{H}_1$$

because diagonal matrices commute. Thus the diagonal component of $\widehat{S}$ makes no contribution to the required property and we can choose

$$\widehat{S} = \widehat{P}_l\widehat{S}\widehat{P}_h + \widehat{P}_l\widehat{S}\widehat{P}_h$$

Now we study the new Hamiltonian in (4), ensuring that it is indeed diagonal in the proper sectors. The first term is obviously diagonal, so the second term is of interest. We have presumed $\widehat{H}_1$ to be off-diagonal, so we can write the commutator as

$$\begin{aligned}[\widehat{S},\widehat{H}_1] =& [\widehat{P}_h\widehat{S}\widehat{P}_l + \widehat{P}_l\widehat{S}\widehat{P}_h, \widehat{P}_h\widehat{H}_1\widehat{P}_l + \widehat{P}_l\widehat{H}_1\widehat{P}_h] \\ =& [\widehat{P}_h\widehat{S}\widehat{P}_l, \widehat{P}_h\widehat{S}\widehat{P}_l] + [\widehat{P}_l\widehat{S}\widehat{P}_h, \widehat{P}_h\widehat{S}\widehat{P}_l] + [\widehat{P}_l\widehat{S}\widehat{P}_h, \widehat{P}_l\widehat{S}\widehat{P}_h] + [\widehat{P}_h\widehat{S}\widehat{P}_l, \widehat{P}_l\widehat{S}\widehat{P}_h]\end{aligned}$$

Under the assumptions that the spaces are orthogonal, the first and third terms vanish to leave us with

$$[\widehat{S},\widehat{H}_1] = \widehat{P}_l\widehat{S}\widehat{P}_h^2\widehat{H}_1\widehat{P}_l - \widehat{P}_h\widehat{H}_1\widehat{P}_l^2\widehat{S}\widehat{P}_h + \widehat{P}_h\widehat{S}\widehat{P}_l^2\widehat{H}_1\widehat{P}_h - \widehat{P}_l\widehat{H}_1\widehat{P}_h^2\widehat{S}\widehat{P}_l$$

which is manifestly a block-diagonal operator: we have removed terms leading to transitions between high and low energy states.

We've shown that the Schrieffer-Wolff transformation works as intended and now it only remains to find an appropriate $\widehat{S}$. As it turns out, one can use

$$\widehat{S} = \frac{1}{U}(\widehat{T}_+ - \widehat{T}_-).$$

which can easily be shown to satisfy (3) using (1). Now substitute the $\widehat{T}_m$ and this newfound generator $\widehat{S}$ into (4). Using (1) we obtain

$$\widehat{H}' = \widehat{V} + \widehat{T}_0 + \frac{1}{U}\Big([\widehat{T}_+, \widehat{T}_-] + [\widehat{T}_0, \widehat{T}_-] + [\widehat{T}_+, \widehat{T}_0]\Big) + O(\widehat{H}_1^3).$$

To make progress we will narrow down our problem to the case of half-filling with two-sites, and "project" onto the low energy sector heuristically. With half-filling, we cannot perform a (single) hop which preserves occupation number since there are no sites without any occupation. Then we can discard any appearances of $\widehat{T}_0$. Without any doubly occupied sites, $\widehat{V}$ (which counts said number) will always produce zero and $\widehat{T}_-$ will vanish acting on any state (we cannot decrease from zero). A tremendous simplification is incurred and we obtain the effective Hamiltonian

$$\widehat{H}_{\text{eff}} = -\frac{1}{U}\widehat{T}_-\widehat{T}_+.$$

This Hamiltonian turns out to have a profound physical interpretation. We can read the transition $\widehat{T}_-\widehat{T}_+$ (which raises then immediately lowers the double occupation number) as a *virtual excitation* with a lifetime too short to be considered physical.[6] Such an excitation, in the low energy regime, manifests itself as a fluctuation in spin wavefunction. With this, we start considering the effect of the virtual excitations on the spin states of the two electrons in the system.

The Pauli exclusion principle prevents electrons with the same spin state from leaving their sites, so we have

$$\widehat{H}_{\text{eff}}\,|\uparrow\uparrow\rangle = 0, \quad \widehat{H}_{\text{eff}}\,|\downarrow\downarrow\rangle = 0 \tag{5}$$

In the case of opposite spins, the two electrons may shuffle around (at the cost of two factors of the kinetic parameter t) such that

$$\langle\uparrow\downarrow|\,\widehat{H}_{\text{eff}}\,|\uparrow\downarrow\rangle = \langle\downarrow\uparrow|\,\widehat{H}_{\text{eff}}\,|\downarrow\uparrow\rangle = 2\frac{t^2}{U} \quad \text{(spin configuration unchanged)} \tag{6}$$

$$\langle\uparrow\downarrow|\,\widehat{H}_{\text{eff}}\,|\downarrow\uparrow\rangle = \langle\downarrow\uparrow|\,\widehat{H}_{\text{eff}}\,|\uparrow\downarrow\rangle = -2\frac{t^2}{U} \quad \text{(spin configuration permuted)} \tag{7}$$

The factor of two arises from the possibility of the virtually doubly-occupied site being either site 1 or 2; i.e., there are two possible manners in which the particles can switch sites, as depicted in Figure 2. Meanwhile the difference in sign simply arises from the anti-commutativity of the fermionic creation and annihilation operators: the choice and order of operators will depend on whether we are permuting the states.

The last step is to express the behavior of the effective Hamiltonian in terms of Pauli operators. It is clear that if the two particles are in the same spin state, the state should be annihilated. Thus we can start with a term

$$\widehat{\sigma}_1^z\widehat{\sigma}_2^z - 1$$

which captures (5). If the spin states are opposite, we obtain an eigenvalue of 2 with the state unchanged; thus we multiply this term by $-t^2/U$ and readily obtain the behavior of (6). The last piece is the ability to turn $|\uparrow\downarrow\rangle$ into $|\downarrow\uparrow\rangle$ and vice versa, as written in (7). This is achieved with the spin lowering and raising operators. The naive answer

$$2\frac{t^2}{U}[\widehat{\sigma}_1^-\widehat{\sigma}_2^+ + \widehat{\sigma}_1^+\widehat{\sigma}_2^-]$$

works because the state is annihilated when we raise a spin-up state or lower a spin down state. In aggregate,

$$\widehat{H}_{\text{eff}} = 2\frac{t^2}{U}\left[\widehat{\sigma}_1^-\widehat{\sigma}_2^+ + \widehat{\sigma}_1^+\widehat{\sigma}_2^- - \frac{1}{2}(\widehat{\sigma}_1^z\widehat{\sigma}_2^z - 1)\right]$$

Using the appropriate Pauli operator identities, we at last obtain

$$\widehat{H} = \frac{t^2}{U}[\widehat{\boldsymbol{\sigma}}_1 \cdot \widehat{\boldsymbol{\sigma}}_2 - 1] = J\widehat{\mathbf{S}}_1 \cdot \widehat{\mathbf{S}}_2 - C, \quad J = \frac{4t^2}{\hbar^2 U}, \quad C = -\frac{t^2}{U}$$

[6] With such a state not being an eigenstate of the effective Hamiltonian, it has a nonzero fluctuation in energy and thus the energy-time relation constrains its lifetime significantly. My understanding is that in the high-energy sector such a state could indeed be an energy eigenstate, and that its virtuality comes from our choice of low-energy regime.

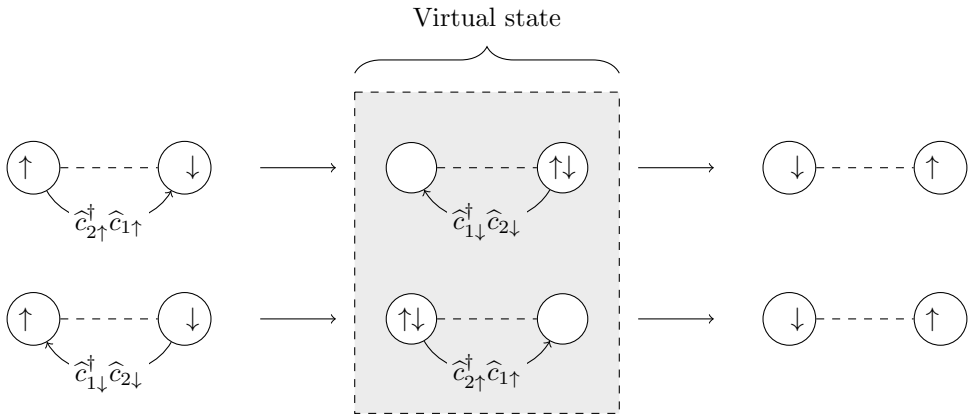

Figure 2: Two possible transitions leading to electron exchanges. Note the doubly-occupied virtual state boxed in gray.

This rewriting continues to hold if we append more sites to either side of the lattice; in this way we obtain exactly our Heisenberg spin chain

$$\hat{H} = J \sum_{\langle ij \rangle} \hat{\mathbf{S}}_i \cdot \hat{\mathbf{S}}_j + \text{constant}$$

where the constant is conventionally dropped out. As promised, we have transfigured the Hubbard model into a Heisenberg spin chain. One might take issue with the sign of J as it restricts us to an antiferromagnetic spin chain; that said, it is now understood that *superexchange* processes can result in *ferromagnetic* effective J-couplings. Thus, we have a good argument that, remarkably, macroscopic magnetism emerges entirely from exchange statistics and Coulomb repulsions, *absent magnetic interactions*.

4 The Density Matrix Renormalization Group

Now that we have defined and properly studied the origins of the Heisenberg spin chain, we use it as a case study for a numerical method which has quickly risen in popularity for tackling spin chains and one-dimensional systems in general. The method is S. R. White's celebrated density matrix renormalization group (DMRG) approach [11], which itself is a modification of the (less accurate) numerical renormalization group.

As initially introduced, DMRG works iteratively in the following manner:

1. We start with two uncoupled, equally sized "blocks", L and R, each of which may contain several coupled sites. Set some parameter D for the maximum dimensionality of our composite Hilbert space for each block, and assume that the dimensionality of each site's Hilbert space is d.

2. Add one site coupled to the right of L and another coupled to the left of R, then couple the enlarged L' and R' to one another to form a *superblock*. Since we're assuming the dimensionality of each block is D, and we've tacked on an additional site to each block, the dimensionality of the superblock Hamiltonian is D^2d^2 (i.e., it is constant in the number of lattices).

3. Diagonalize this Hamiltonian and obtain its groundstate and groundstate energy. If we're satisfied with the number of iterations, return this value.

4. If we're proceeding, we will pick L' and R' as the new L and R in the following iteration; however, in order to tame the dimensionality of the Hilbert spaces of these growing blocks (i.e., begin the next iteration with D-dimensional blocks), we will need to perform some sort of projection from Dd-dimensions onto a suitably chosen D-dimensional subspace. This is the pith of White's insight:

the numerical renormalization group technique would pick the D-lowest energy eigenstates of the Hamiltonian and project onto that subspace; instead, we will be informed by the intuition that *the most relevant states should be the (classically) most likely states of the reduced density matrix of either block*. Thus, we pick the groundstate of the superblock Hamiltonian and take the partial trace of its density matrix with respect to the right enlarged block in order to obtain the reduced density matrix of the left enlarged block, diagonalize this reduced density matrix, and pick the D highest-eigenvalue states as the basis for the new subspace.[7] These will form a $Dd \times D$ change of basis matrix which we will call $\widehat{P}$.

5. Transform all involved operators according to the projection onto this subspace: any operator $\widehat{A}$ will become $\widehat{A}' = \widehat{P}^\dagger \widehat{A} \widehat{P}$ (n.b. the dimensionality of $\widehat{A}$ is not the same as that of $\widehat{A}'$). This step is crucial as it will allow us to transform the operators that will be involved in the coupling between the blocks and the appended sites in order to form the enlarged L' and R' in the next iteration.

6. Repeat.

4.1 DMRG in Context of Matrix Product States

The above description is suitable as pedagogical explanation for DMRG's efficacy, but is now considered an outdated approach to the algorithm. We now understand that the method works well because it can be regarded as a variational method in the subspace of *matrix product states* [8], which themselves are a particular form in the broader field of tensor network theory. Put briefly, the chief tenet of tensor network theory is the expression wavefunctions in the form

$$|\psi\rangle = \sum_{i_1,\ldots,i_N} \Psi_{i_1,\ldots,i_N} |i_1\rangle \otimes \cdots \otimes |i_N\rangle$$

where $\Psi_{i_1,\ldots i_N}$ is a rank N tensor which can be written as some carefully chosen *contraction of other tensors*; these tensors and their contracting indices form a *tensor network*. Such states are advantageous because they dramatically decrease the order of the number of parameters,[8] thereby dramatically restricting the relevant sector of the Hilbert space, and because connecting indices *represent wavefunction correlations*, allowing us to study entanglement in a more geometric light [7]. To make this concrete, let us take the class of tensor operator states relevant in the spin chain context, the matrix product states (MPS):

$$|\psi\rangle = \sum_{\sigma_1,\ldots,\sigma_L} \Psi_{\sigma_1,\ldots,\sigma_L} |\sigma_1,\ldots,\sigma_L\rangle\,, \quad \text{with} \quad \Psi_{\sigma_1,\ldots,\sigma_L} = \sum_{a_1,\ldots,a_{L-1}} A^{\sigma_1}_{a_1} A^{\sigma_2}_{a_1,a_2} \cdots A^{\sigma_{L-1}}_{a_{L-2},a_{L-1}} A^{\sigma_L}_{a_{L-1}}$$

Here each $A^{\sigma_i}_{a_j,a_k}$ represents a matrix and the first and last matrices are merely vectors (explaining the "matrix product" nomenclature). Then we can see how writing the state in this way may elucidate the lattice geometry's effect on the entanglement in the system: Open indices in the tensor network formalism correspond to the physical degrees of freedom; thus, choosing a particular σ_1 has immediate effects on the matrix product $A^{\sigma_1}_{a_1} A^{\sigma_2}_{a_1,a_2}$, (in turn affecting the particular values of σ_2 that may be found with that given σ_1) but also, through the sequence of matrix multiplications, an effect on sites as far as σ_L *mediated* by the in-between matrices for σ_j with $2 < j < L$. This point is graphically punctuated by *tensor network diagrams* such as that in Figure 3.

Given the nearest-neighbor nature of the spin chain's couplings, we expect the MPS to be an appropriate form for the groundstate of a spin chain. Indeed, it is a remarkable fact that S. R. White's physically motivated renormalization is actually formally equivalent to a *truncated singular value decomposition*[9] that gives rise to a MPS form of the groundstate wavefunction. In fact, DMRG works to great accuracy because the

[7] Recall that the eigenvalues of the density matrix roughly correspond to classical probabilities for finding the ensemble in the corresponding eigenstate.

[8] Specifically, to polynomial order in the rank of the contracted tensor and the maximum number of indices of the tensors in the network.

[9] Truncated SVD is coincidentally a common dimensionality reduction technique in data science. In fact, many streaming services use it to recommend movies or music based on sparse data.

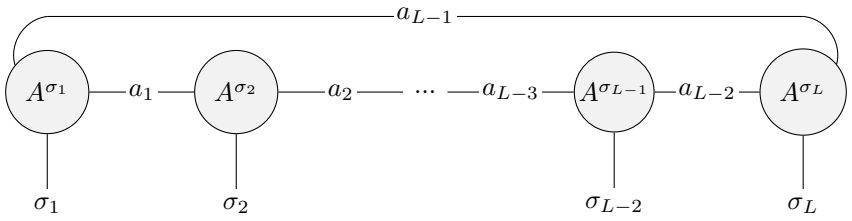

Figure 3: The tensor network diagram for an MPS with periodic boundary conditions. Notice the edges in the graph are the connecting indices between the tensors. Also notice that the lower indices are omitted in A^{σ_i}.

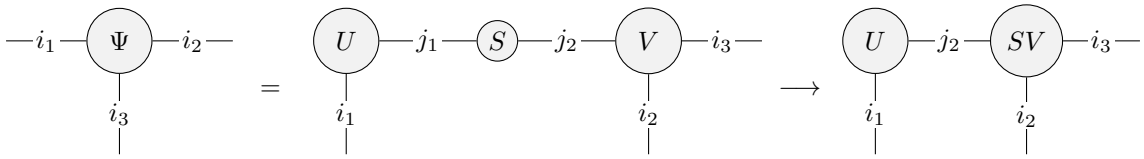

Figure 4: Restoration of MPS form of Ψ through SVD as given in (8-10). Note that the last step represents truncated matrices.

singular value decomposition successfully minimizes the 2-norm (Frobenius norm) of the difference between the projected (truncated, or renormalized) density matrix and the larger-dimensional density matrix [9]

$$\widehat{P}\widehat{\rho}\widehat{P}^{\dagger} = \widehat{\rho}' \Longrightarrow \min ||\widehat{\rho} - \widehat{\rho}'||$$

The SVD works within MPS subspace in the sense that the renormalization procedure restores the MPS form of the candidate eigenstate at every iteration of the algorithm. In particular, under the assumption that the Hamiltonian is itself expressible as a matrix product (which is the case for spin chain Hamiltonians), modern implementations of DMRG find the groundstate of the superblock Hamiltonian by using a trial MPS, carefully contracting indices up to the newly appended sites, and subsequently employing a variational method on the MPS of the new sites with respect to the contracted Hamiltonian (typically one uses the Davidson or Lanczos algorithm). This produces a new state

$$|\psi\rangle = \sum_{i_1,i_2,i_3} \Psi_{i_1,i_2,i_3} |i_1, i_2, i_3\rangle , \tag{8}$$

performing a SVD:

$$\Psi_{i_1,i_2,i_3} = \sum_{j_1,j_2} U^{i_1}_{j_1} S_{j_1,j_2} V^{i_2,i_2}_{j_2}, \tag{9}$$

then subsequently truncating the SVD and contracting to obtain

$$\Psi_{i_1,i_2,i_3} = \sum_{j_1} U^{i_1}_{j_1} (SV)^{i_2,i_2}_{j_1}. \tag{10}$$

The crucial feature to understand in this procedure is that the states in (8) and (9) are *not* necessarily MPSs, but the truncated tensor above *is*; Figure 4 illustrates this. One then continues this procedure for the remaining tensors in the MPS, eventually optimizing the entire candidate state and achieving an approximation of the groundstate. If we continue growing the spin chain (until a desired length is reached or until the groundstate is translationally invariant), the algorithm described above is termed the infinite DMRG or iDMRG. On the other hand, if we are interested in a *finite* spin chain, the algorithm will start with some fixed-length trial groundstate and "sweep" the chain, growing the right half of the chain while shrinking the left, then repeating the process in the reverse direction [10].

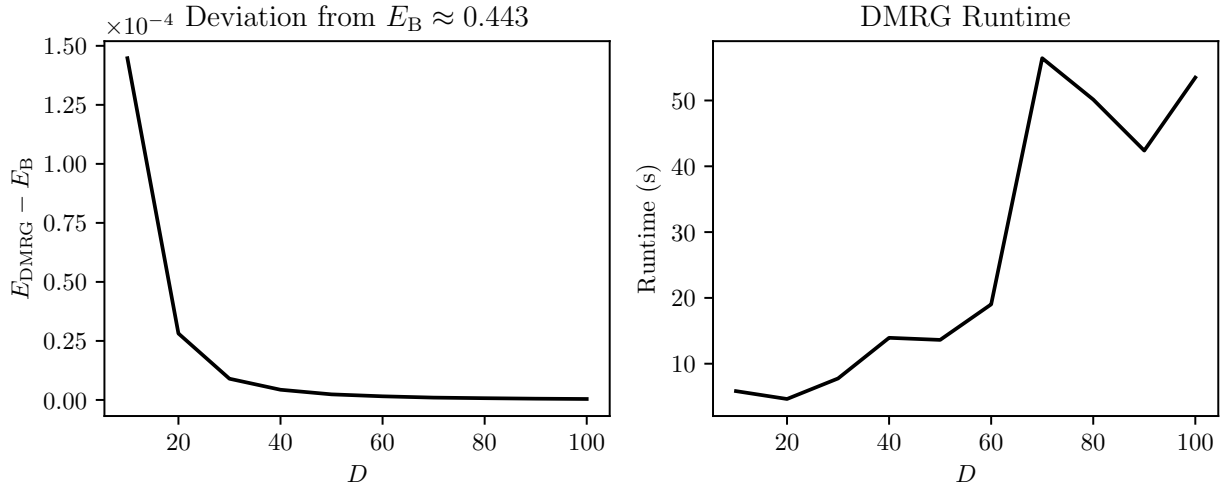

Figure 5: (Left) The groundstate energy per site as calculated by DMRG, E_{DMRG}, as compared to the Bethe ansatz groundstate energy $E_{\text{B}} \approx -0.4431$ for varying truncated dimensions D. We can see that even at low D the DMRG energy converges to a value within 10^{-3} of the Bethe ansatz value. (Right) The runtimes for the DMRG algorithm in seconds with varying D. As expected, the runtime increases with D as the Hamiltonian diagonalization procedure becomes exponentially more complex.

It is worth noting that the SVD matrices are related to the density matrix diagonalization procedure outlined above by

$$|\psi\rangle\langle\psi| = \sum_{k_1,k_2} \Psi'_{k_1,k_2} |k_1\rangle\langle k_2| , \quad \Psi'_{k_1,k_2} = \sum_{j_1,j_2} U^{k_1}_{j_1} S^2_{l_1,l_2} (U^\dagger)^{k_2}_{l_2}$$

where we've obtained this form by multiplying (9) by its Hermitian conjugate and using the fact that the SVD produces a diagonal S and unitary V.

A more throughout description of the DMRG in the MPS language is beyond the scope of this paper and can be found in [10]. An excellent outline of the finite version of the algorithm using tensor network diagrams can be found in [1].

4.2 DMRG on a Heisenberg Spin Chain

The Heisenberg spin chain is a good model to test DMRG against because it admits a well-known analytical solution, the *Bethe ansatz*. With that, we will compare the Bethe ansatz groundstate energy to a solution obtained through DMRG to find that indeed the method works to surprising accuracy. The Bethe ansatz predicts a groundstate energy per site of [6]

$$E_{\text{B}} = \frac{1}{4} - \ln 2 \approx -0.4431.$$

Using the tensor network Python package TeNPy [4] we run ten iDMRGs with varying truncated dimensions D ranging from 10 to 100 at intervals of 10 on a Heisenberg XXX spin chain. The resulting energies per unit site are plotted alongside the algorithm runtimes in Figure 5. Note that the TeNPy DMRG implementation runs the algorithm until a convergence criterion is met. A Jupyter notebook containing the script used to run these simulations can be found here.

5 References

[1] Density matrix renormalization group algorithm. https://tensornetwork.org/mps/algorithms/dmrg/. Accessed: 2022-06-1.

[2] Sergey Bravyi, David P. DiVincenzo, and Daniel Loss. Schrieffer–wolff transformation for quantum many-body systems. *Annals of Physics*, 326(10):2793–2826, oct 2011.

[3] S.M. Girvin and K. Yang. *Modern Condensed Matter Physics*. Cambridge University Press, 2019.

[4] Johannes Hauschild and Frank Pollmann. Efficient numerical simulations with Tensor Networks: Tensor Network Python (TeNPy). *SciPost Phys. Lect. Notes*, page 5, 2018. Code available from https://github.com/tenpy/tenpy.

[5] Daichi Hirobe, Takayuki Kawamata, Koichi Oyanagi, Yoji Koike, and Eiji Saitoh. Generation of spin currents from one-dimensional quantum spin liquid. *Journal of Applied Physics*, 123(12):123903, 2018.

[6] Michael Karbach, Kun Hu, and Gerhard Müller. Introduction to the bethe ansatz II. *Computers in Physics*, 12(6):565, 1998.

[7] Román Orús. A practical introduction to tensor networks: Matrix product states and projected entangled pair states. *Annals of Physics*, 349:117–158, oct 2014.

[8] Stefan Rommer and Stellan Östlund. Class of ansatz wave functions for one-dimensional spin systems and their relation to the density matrix renormalization group. *Physical Review B*, 55(4):2164–2181, jan 1997.

[9] U. Schollwöck. The density-matrix renormalization group. *Reviews of Modern Physics*, 77(1):259–315, apr 2005.

[10] Ulrich Schollwöck. The density-matrix renormalization group in the age of matrix product states. *Annals of Physics*, 326(1):96–192, jan 2011.

[11] Steven R. White. Density-matrix algorithms for quantum renormalization groups. *Phys. Rev. B*, 48:10345–10356, Oct 1993.